Realisation of Hybrid Trapped Field Magnetic Lens (HTFML) consisting of REBCO bulk lens and REBCO bulk cylinder at 77 K

S Namba[1], H Fujishiro[1], T Naito[1], M D Ainslie[2] and D Zhou[3]

[1] Department of Physical Science and Materials Engineering, Faculty of Science and Engineering, Iwate University, 4-3-5 Ueda Morioka, Japan
[2] Bulk Superconductivity Group, Department of Engineering, University of Cambridge, Trumpington Street, Cambridge CB2 1PZ, UK
[3] Department of Physics, Shanghai University, Shanghai, 200444, China

E-mail: g0318128@iwate-u.ac.jp

Abstract. A hybrid trapped field magnet lens (HTFML) can reliably generate a concentrated magnetic field, B_c, in the centre of the magnetic lens higher than the trapped field of the trapped field magnet (TFM) and the applied magnetic field, B_{app}, even after the external magnetizing field decreased to zero. In this paper, the performance of HTFMLs consisting of EuBaCuO bulk TFM with various heights and a GdBaCuO bulk magnetic lens was investigated at 77 K using liquid nitrogen. A concentrated magnetic field of B_c = 0.80 T was achieved at the centre of the HTFML for the tallest TFM after removing an applied magnetic field of B_{app} = 0.50 T. The influence of the height of the outer TFM cylinder on the final concentrated field was studied experimentally and discussed using numerical simulation.

1. Introduction

REBaCuO (where RE is rare earth element or Y) bulk superconductors have a potential to trap magnetic fields much higher than that of a conventional Nd-Fe-B magnet. Thus, the magnetized REBaCuO bulk can be used as a promising compact, high-strength trapped field magnet (TFM) for many engineering applications. The world record magnetic field of 17.6 T at 26 K was achieved in a GdBaCuO disk pair reinforced by shrink-fit stainless steel [1]. Furthermore, the trapped field of 4.3 T was generated in a GdBaCuO disk pair even at 77 K [2]. An EuBaCuO ring-shaped bulk superconductor is suitable for practical applications such as a nuclear magnetic resonance (NMR) spectrometer and magnetic resonance imaging (MRI) equipment because of its low relative magnetic permeability (μ_r = 1.0013), compared with that of GdBaCuO (μ_r = 1.0194) [3–5].

In addition, a ‘magnetic lens’ using cone-shaped bulk superconductors has been investigated, in which a magnetic field is concentrated in the bore of the lens using the ‘diamagnetic shielding effect’ of superconducting materials and the magnetic field in the lens is higher than the applied field generated by an external magnetizing coil [6–11]. A higher concentrated field of B_c = 12.42 T has been achieved at 20 K for a background field of B_{app} = 8 T using a bulk GdBaCuO lens [6]. Using an MgB_2 magnetic lens, B_c = 2.1 T was also achieved at 17 K for B_{app} = 1 T [12].

We proposed a new concept of a hybrid trapped field magnet lens (HTFML) in 2018, which consists of a TFM cylinder exploiting the ‘vortex pinning effect’, combined with a bulk magnetic lens

exploiting the 'diamagnetic shielding effect' [13]. The HTFML can reliably generate a concentrated magnetic field in the centre of the magnetic lens higher than the trapped field of the TFM and the applied magnetic field, even after the external magnetizing field decreases to zero. Very recently, we confirmed the experimental realization of the HTFML using a GdBaCuO magnetic lens and MgB_2 TFM cylinder [14], in which a maximum concentrated magnetic field of B_c = 3.55 T was achieved at the central bore of the HTFML device after removing the applied field of B_{app} = 2.0 T at T = 20 K.

It is better for the HTFML consisting of both REBaCuO magnetic lens and TFM cylinder to achieve higher HTFML effect. In this paper, the performance of HTFML consisting of a GdBaCuO bulk magnetic lens and EuBaCuO bulk TFM cylinder was investigated at 77 K using a liquid nitrogen.

2. Experimental Procedure

Figure 1 shows the experimental setup for the HTFML device. As outer bulk cylinder, three ring-shaped EuBaCuO bulks were stacked (TFM-A, B and C), which were fabricated by QMG^{TM} method by Nippon Steel Corporation, Japan [15]. The dimension of the TFM-A and C is 60 mm in outer diameter (OD), 36 mm in inner diameter (ID) and 17 mm in height (H). The TFM-B is 60 mm in OD, 36 mm in ID and 20 mm in H. Each EuBaCuO ring bulk was reinforced by an Al alloy ring 5 mm in thickness (70 mm in OD, 60 mm in ID) with the same height of each bulk, which is a suitable material for the reinforcement of the bulk applied to NMR apparatus because of non-magnetic and higher mechanical strength [3]. A GdBaCuO magnetic lens was prepared by the following process: stacked double GdBaCuO cylindrical bulks (OD = 36 mm, ID = 10 mm, H = 30 mm) fabricated by QMG^{TM} method were machined into a cone-shaped lens (OD = 30 mm, ID = 10 mm, ID2 = 26 mm, outer height (OH) = 30 mm and inner height (IH) = 8 mm), as shown in Fig. 1(b). The dimensions of the bulk lens were optimized using numerical simulations [16]. Thin slits 200 μm in width were made to disrupt the circumferential flow of the shielding current during the zero-field-cooled magnetization (ZFCM) process. The GdBaCuO magnetic lens was encapsulated in a stainless steel (SS) holder to prevent mechanical fracture from the Lorentz force. The time evolution of the concentrated magnetic field, B_c, at the central bore of the HTFML was measured by an axial-type Hall sensor (F. W. Bell, BHA-921). The similar experiments were performed for the case of double TFMs (TFM-A and B) and single TFM (TFM-B).

Since magnetic lens and TFM cylinder are made of the similar REBaCuO materials, an individual temperature control is necessary to realize the HTFML effect. Figure 2 shows the time sequence of the external magnetic field, B_{ex}, and the temperatures, T, of the EuBaCuO TFM cylinders and GdBaCuO magnetic lens during the magnetizing procedure, which comprises the following five stages.

(1) The long outer glass fibre reinforced plastic (GFRP) container (96 mm in OD, 80 mm in ID) was set in the room temperature bore (100 mm in diameter) of the cryocooled superconducting solenoid magnet (170 mm in OD, 120 mm in ID, 200 mm in H, JASTEC JMTD-10T100). The GdBaCuO magnetic lens encapsulated by SS holder was set in the inner GFRP container (35 mm in OD, 33 mm in ID), and was placed at the centre of the outer GFRP container. The liquid nitrogen was poured into both GFRP containers.

(2) The external magnetic field, B_{ex}, was linearly ramped up to the maximum magnetic field of B_{app} = 0.50 T at +0.222 Tmin^{-1}. This process corresponds to ZFCM for the GdBaCuO lens, in which the magnetic field at the central position is higher than B_{app} because of the shielding effect by the magnetic lens.

(3) After B_{ex} reached to B_{app} = 0.50 T, the EuBaCuO TFMs in the plastic container were immersed slowly to the bottom of the outer GFRP container filled with liquid N_2.

(4) B_{ex} was decreased linearly at −0.222 Tmin^{-1} down to zero. During this process, the outer EuBaCuO TFMs were magnetized by field-cooled magnetization (FCM) and magnetic flux was trapped. A magnetic field at the centre of the magnetic lens still remains due to the existence of the trapped field in the EuBaCuO TFMs.

(5) As a result, the HTFML can reliably generate a magnetic field higher than the trapped field in the EuBaCuO TFMs and B_{app}, even after B_{ex} = 0.

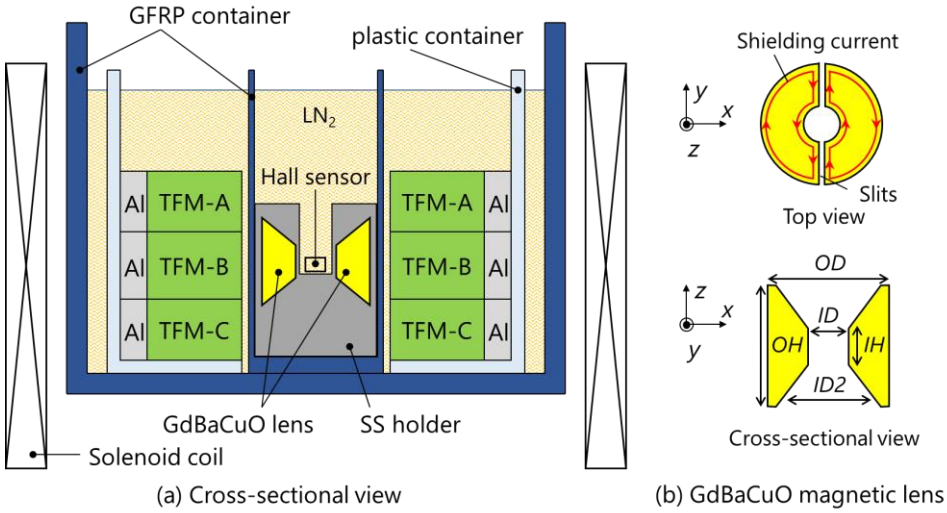

Figure 1. (a) The schematic illustration of the experimental setup for the HTFML using liquid nitrogen, which corresponds to the magnetizing stage of (3) (see text). (b) Cross-sectional and top views of the GdBaCuO magnetic lens with slits. When a magnetic field is applied to the lens along the +*z*-direction, the shielding current flows like red arrows and the magnetic flux penetrates into the bore of the lens through the slits. As a result, the magnetic field along the +*z*-direction is amplified due to the shielding current.

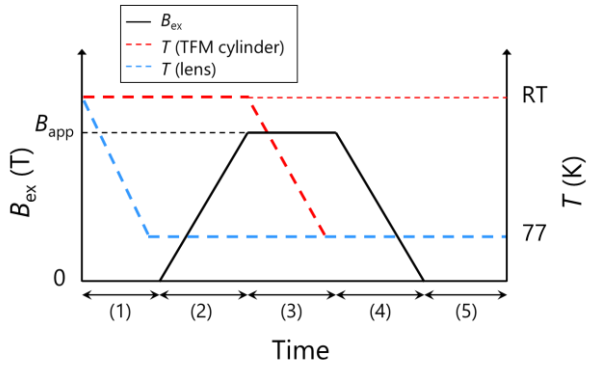

Figure 2. Time sequence of the external magnetic field, B_{ex}, at the centre of the HTFML and the temperatures, T, of the EuBaCuO TFMs and GdBaCuO magnetic lens during the magnetizing procedure.

3. Numerical simulation

Based on the experimental setup of the HTFML as shown in Fig. 1, a three-dimensional numerical simulation model was constructed, which consists of the bulk magnetic lens, bulk cylinders and a magnetizing solenoid coil. The magnetic lens and solenoid coil were assumed to be the same size as those used in the experiments. The magnetic lens has two slits with 5 deg. along the *y*-direction. All bulk TFMs were assumed to be the same size of 60 mm in OD, 36 mm in ID and 20 mm in H for simplicity. The numerical simulation was carried out using the commercial finite element method software package, Photo-Eddy (Photon Ltd., Japan), which helped us to understand electromagnetic phenomena of HTFML during the magnetization process. The details of fundamental equations for the simulations are described elsewhere [17–19]. The nonlinear relationship between the electric field, E, and current, J, of the superconducting bulk was given by the power–n law (n = 20). The magnetic field dependence of the critical current density, $J_c(B)$, for the bulks used in this simulation was described using the following equation [20–22],

$$J_c(B) = J_{c1}\exp\left(-\frac{B}{B_L}\right) + J_{c2}\frac{B}{B_{max}}\exp\left[\frac{1}{k}\left(1-\left(\frac{B}{B_{max}}\right)^k\right)\right], \quad (1)$$

where J_{c1}, J_{c2} are magnitudes of the central and secondary peaks, respectively: B_{max} is the secondary peak position, B_L and k are coefficients. These free fitting parameters, J_{c1}, B_L, J_{c2}, B_{max} and k in equation (1) for the EuBaCuO TFM cylinders and GdBaCuO magnetic lens are shown in table 1, which reproduced the experimental results of the time evolution of the measured magnetic field during FCM for the single EuBaCuO TFM (TFM-B) and ZFCM for the single GdBaCuO magnetic lens, respectively.

Table 1. Fitting parameters of the $J_c(B)$ characteristics for the EuBaCuO TFM cylinder and GdBaCuO magnetic lens, shown in eq. (1).

	J_{c1} (A m^{-2})	B_L (T)	J_{c2} (A m^{-2})	B_{max} (T)	k
EuBaCuO TFM cylinder	5.9×10^8	0.4	1.8×10^9	1.7	2.4
GdBaCuO magnetic lens	7.2×10^8	0.4	2.2×10^9	1.7	2.4

4. Results and discussion

4.1. FCM for single GdBaCuO cylinder and ZFCM for single GdBaCuO lens

Figure 3(a) shows experimental and simulation results of the time dependence of the trapped field, B_c, at the centre of the single TFM (TFM-B) and the external field, B_{ex}, during FCM, ramped down from 1.0 T at 77 K. The experimental B_c value of 0.82 T was trapped finally after the flux creep in the descending stage, which suggested the trapped field ability of the TFM-B at 77 K. The simulation curve of the field-dependent B_c reproduced the experimental one.

Figure 3(b) shows the experimental and simulation results of the time dependence of the magnetic field, B_c, at the centre of the single GdBaCuO lens and the external field, B_{ex}, during the magnetizing process of HTFML for B_{app} = 0.50 T at 77 K. The effect of magnetic field concentration by the magnetic lens was confirmed experimentally. The negative magnetic field of B_c was observed after the magnetization, which resulted from the magnetic flux penetration into the bulk lens. Just after the ascending stage in the simulation, the concentrated magnetic field sharply increased, which is in clear contrast to the experimental result. This discrepancy originates from the width of slits gap. In the simulation, slit gap is 5 deg., which is wider than the actual slit gap. Therefore, more magnetic flux generated by the external magnetizing coil is intruded in the lens bore, compared to the situation. However, simulated B_c gradually decreased with time and was nearly the same as experimental one in the descending stage and after magnetization.

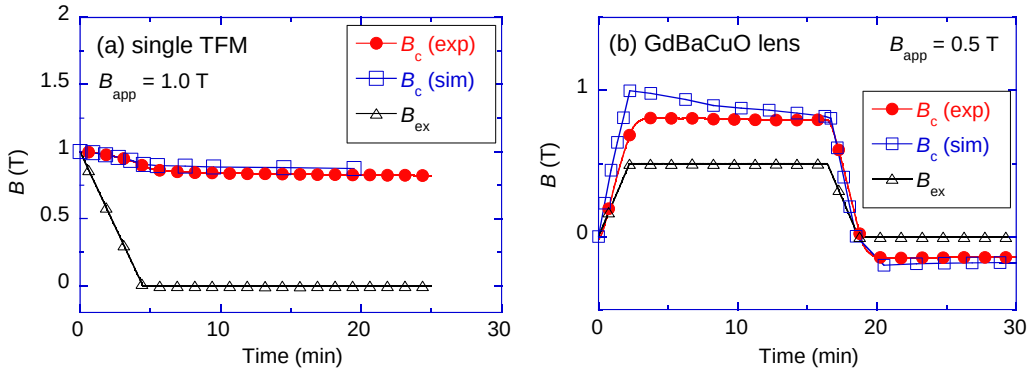

Figure 3. Experimental results of the time dependence of measured magnetic field, B_c, for (a) the single EuBaCuO bulk cylinder (TFM-B) during FCM from B_{app} = 1.0 T at 77 K, and for (b) the single GdBaCuO magnetic lens during HTFML magnetizing process, shown in Fig. 1, for B_{app} = 0.5 T at 77 K. The simulation results of B_c are also shown in each figure.

4.2. Comparison of FCM for triple, double and single EuBaCuO TFMs

Figures 4(a) - 4(c), respectively, show the time evolution of the measured magnetic field, B_c, at the centre of the triple, double and single EuBaCuO TFM and external field, B_{ex}, during the HTFML magnetization process for B_{app} = 0.50 T. In the ascending stage, the magnetic field, B_c, increased linearly with increasing B_{ex} and the magnitude of B_c was the same as the external field because the EuBaCuO cylinders were in the normal state. In the descending stage, in which the bulk cylinders were cooled in liquid N_2 and then FCM was performed, the final trapped field of the triple and double EuBaCuO TFMs was 0.50 and 0.49 T, respectively. For the single TFM (TFM-B), as shown in Fig. 4(c), a small amount of flux flow was observed and the final trapped field was decreased to B_c = 0.46 T.

Figure 5 shows the numerical simulation results of magnetic field, B_c, at the centre of the triple, double and single EuBaCuO TFMs and external field, B_{ex}, during the magnetizing process for B_{app} = 0.50 T at 77 K. Final trapped field of these cases at 35 min (after approximately 15 min later from the ramp end) was 0.50, 0.50 and 0.46 T, respectively. For the single TFM, a small flux flow observed experimentally in the descending stage was reproduced in this simulation.

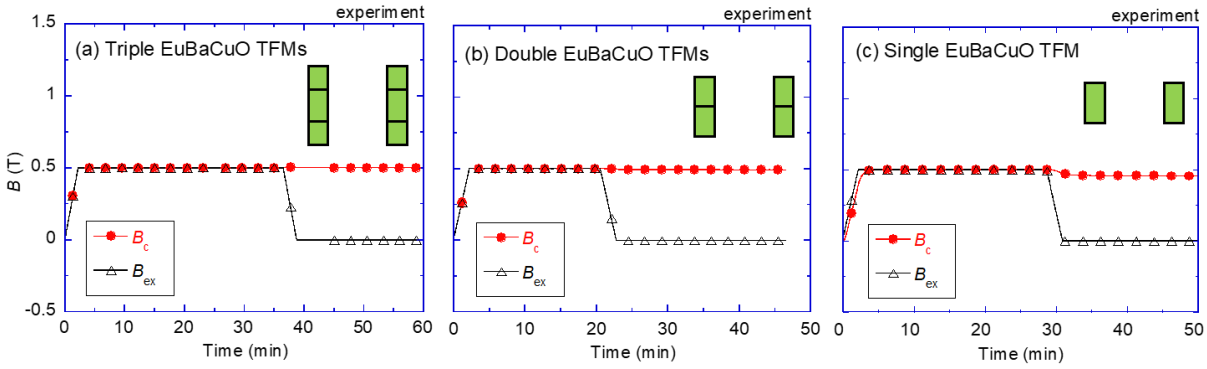

Figure 4. Time evolution of the measured magnetic field, B_c, at the centre of the (a) triple, (b) double and (c) single EuBaCuO TFM at 77 K and external field, B_{ex}, during the magnetization process for B_{app} = 0.5 T.

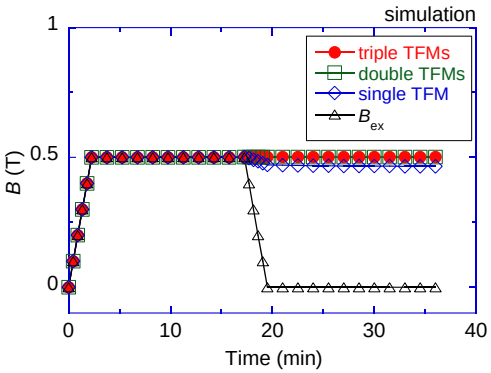

Figure 5. The numerical simulation results of magnetic field, B_c, during the magnetizing process for B_{app} = 0.5 T at the centre of the EuBaCuO cylinder using triple, double and single TFM.

4.3. HTFML effect using triple, double and single EuBaCuO TFM with GdBaCuO lens

Figure 6 presents the confirmation of the HTFML effect consisting of GdBaCuO magnetic lens and EuBaCuO cylinder with triple, double and single TFM during the HTFML magnetization process for B_{app} = 0.50 T. In the ascending stage using triple TFMs, as shown in Fig. 5(a), B_c was higher than B_{ex} due to the diamagnetic shielding effect in the GdBaCuO magnetic lens and then finally B_c = 0.81 T was achieved. In the descending stage, after cooling process, B_c decreased slightly to 0.80 T. This result suggests that the HTFML effect at 77 K was confirmed. However, the final B_c value for the HTFML device using double and single EuBaCuO TFMs was decreased to 0.74 T and 0.56 T, respectively, as shown in Figs. 6(b) and 6(c). Although the trapped field ability for each TFM is almost the same (see Fig. 4), the HTFML effect decreased with decreasing height of the TFM cylinder. In particular, the HTFML effect with the single TFM was less than the other cases.

Figure 7 shows the numerical simulation results of magnetic field, B_c, during the magnetizing process of HTFML for B_{app} = 0.50 T at the centre of the HTFML using triple, double and single EuBaCuO TFMs. Just after the ascending stage, the concentrated magnetic field gradually decreased for all cases due to the gradual magnetic flux penetration into the bulk lens because of the lower $J_c(B)$ characteristics at 77 K. For the use of triple and double EuBaCuO TFMs, in the descending stage, the time dependence of B_c was nearly the same and the final B_c values of 0.77 T were achieved. On the other hand, for the single EuBaCuO TFM case, as shown in Fig. 6(c), an abrupt decrease in B_c can be observed, which was similar to the experimental result, and the final B_c was 0.58 T. These numerical simulation results fairly reproduced the experimental ones as shown in Fig. 6.

Finally, we consider the reason of the difference of the HTFML effect for EuBaCuO cylinder with different height. Figures 8(a) and 8(b) show the simulation results of the final trapped field and magnetic flux line distributions for the HTFML using triple and single TFMs, respectively. The final trapped field for the HTFML using single TFM was B_c = 0.46 T, which was slightly smaller than that using triple TFMs (B_c = 0.50 T), as shown in Fig. 5. The magnetic flux penetration can be confirmed in inner periphery of the bulk lens for each case. The difference of final B_c in the HTFML comes from the route of the magnetic flux concentration into the lens. For the HTFML using triple TFMs, magnetic flux line is along the +z-direction and trapped field generated from the TFMs is concentrated efficiently in the lens. On the other hand, for the HTFML using single TFM, magnetic flux cannot be collected to the lens effectively because the height of TFM (H = 20 mm) is shorter than that of the lens (H = 15 mm). From both simulation and experimental results, the HTFML device should be consisted of TFMs with at least higher than the lens for better HTFML performance.

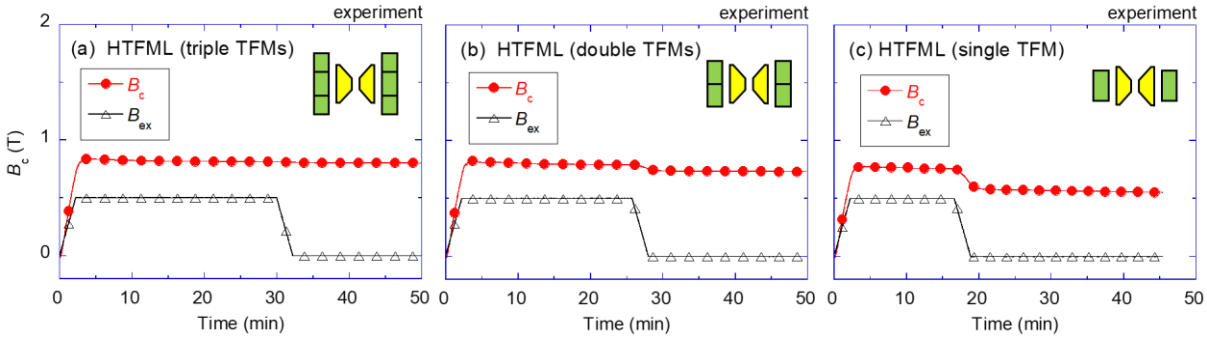

Figure 6. Experimental results of measured magnetic field, B_c, during the magnetizing process for B_{app} = 0.5 T at the centre of the HTFML using (a) triple, (b) double and (c) single EuBaCuO TFM.

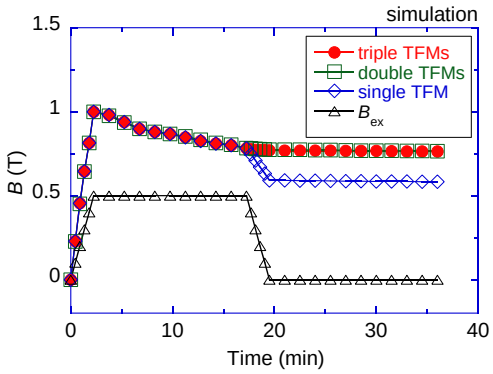

Figure 7. The numerical simulation results of magnetic field, B_c, during the magnetizing process for B_{app} = 0.5 T at the centre of the HTFML using triple, double and single EuBaCuO TFM.

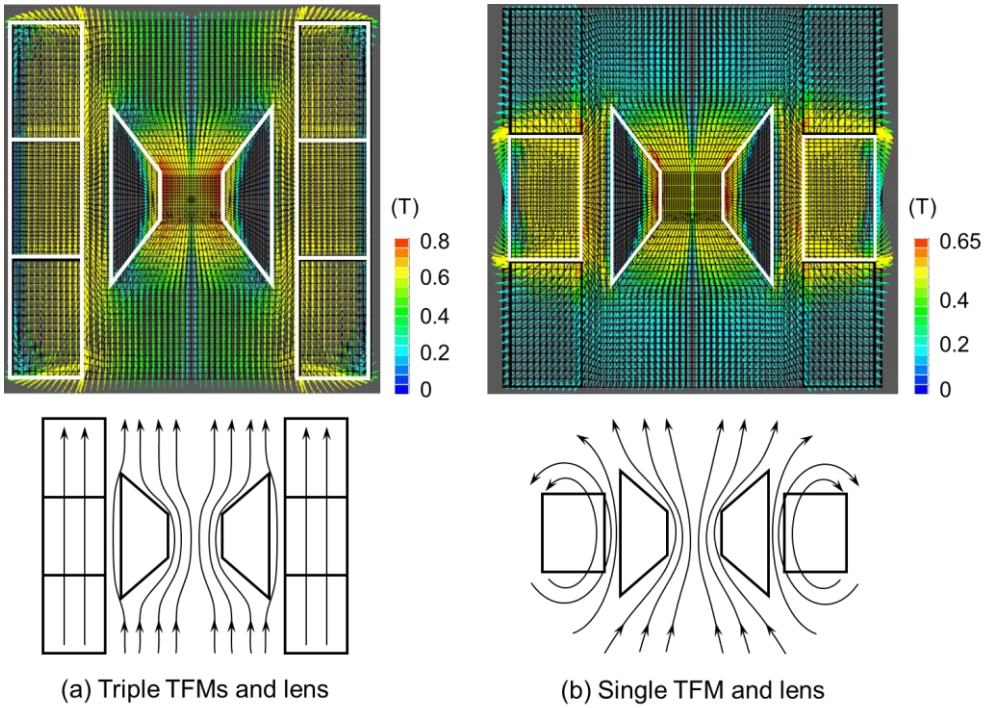

Figure 8. Comparison of final distributions of the magnetic field and magnetic flux lines for the HTFML using (a) triple and (b) single TFM. Schematic view of the magnetic flux distribution is also shown in each case.

5. Summary

The performance of HTFML consisting of EuBaCuO bulk TFMs with various heights and a GdBaCuO bulk magnetic lens was experimentally investigated at 77 K using liquid nitrogen. A concentrated magnetic field, B_c = 0.80 T, at the centre of the HTFML was achieved for the longer TFM after removing an applied magnetic field of B_{app} = 0.50 T. The experimental results were reproduced well by the numerical simulation. The HTFML effect was reduced with decreasing height of EuBaCuO TFM cylinder under the identical GdBaCuO bulk magnetic lens. To enhance the HTFML effect using both REBaCuO bulk TFMs and REBaCuO bulk magnetic lens, it is necessary to lowering the operating temperature.

Acknowledgements

The authors thank Mr. Y. Yanagi of IMRA Material R&D Co., Ltd., Japan, for valuable experimental supports. This research is supported by Adaptable and Seamless Technology transfer Program through Target-driven R&D (A-STEP) from Japan Science and Technology Agency (JST), Grant No. VP30218088419 and by JSPS KAKENHI Grant No. 19K05240. M. D. Ainslie would like to acknowledge financial support from an Engineering and Physical Sciences Research Council (EPSRC) Early Career Fellowship, EP/P020313/1.

References

[1] Durrell J H, Dennis A R, Jaroszynski J, Ainslie M D, Palmer K G B, Shi Y-H, Campbell A M, Hull J, Strasik M. Hellstrom E E and Cardwell D A 2014 *Supercond. Sci. Technol.* **27** 082001
[2] Nariki S, Sakai N and Murakami M 2005 *Supercond. Sci. Technol.* **18** S126–S130
[3] Nakamura T, Tamada D, Yanagi Y, Itoh Y, Nemoto T, Utumi H and Kose K 2015 *J. Magn. Reson.* **259** 68–75
[4] Nakamura T, Itoh Y, Yoshikawa M, Oka T and Uzawa J 2007 *Concepts Magn. Reson.* B **31B** 65–70
[5] Ogawa K, Nakamura T, Terada Y, Kose K and Haishi T 2011 *Appl. Phys. Lett.* **98** 234101
[6] Zhang Z Y, Matsumoto S, Teranishi R and Kiyoshi T 2012 *Supercond. Sci. Technol.* **25** 115012
[7] Choi S, Yoon J-H, Lee B-S, Won M-S, Ok J-W, Zhang Z-Y, Kiyoshi T, Matsumoto S and Lee S-H 2012 *J. Appl. Phys.* **111** 07E728
[8] Kiyoshi T, Choi S, Matsumoto S, Asano T and Uglietti D 2009 *IEEE Trans. Appl. Supercond.* **19** 2174–7
[9] Zhang Z Y, Matsumoto S, Teranishi R and Kiyoshi T 2013 *Supercond. Sci. Technol.* **26** 045001
[10] Asano T, Itoh K, Matsumoto S, Kiyoshi T, Wada H and Kido G 2005 *IEEE Trans. Appl. Supercond.* **15** 3157–60
[11] Choi S, Kiyoshi T and Matsumoto S 2009 *J. Appl. Phys.* **105** 07E705
[12] Zhang Z Y, Choi S, Matsumoto S, Teranishi R, Giunchi G, Albisetti A F and Kiyoshi T 2012 *Supercond. Sci. Technol.* **31** 025009
[13] Takahashi K, Fujishiro H and Ainslie M D 2018 *Supercond. Sci. Technol.* **31** 044005
[14] Namba S, Fujishiro H, Naito T, Ainslie M D and Takahashi K, 2019 submitted to *Supercond. Sci. Technol.*.
[15] Morita M, Sawamura M, Takebayashi S, Kimura K, Teshima H, Tanaka M, Miyamoto K and Hashimoto M 1994 *Physica C* **235–240** 209–12
[16] Namba S, Fujishiro K, Ainslie M D, Takahashi K, Namburi D K, Zhou D and Naito T 2019 *IEEE Trans. Appl. Supercond.* **29** 6801605
[17] Fujishiro H, Itoh Y, Yanagi Y and Nakamura T 2015 *Supercond. Sci. Technol.* **28** 095018
[18] Ainslie M D and Fujishiro H 2015 *Supercond. Sci. Technol.* **28** 053002
[19] Fujishiro H, Naito T, Yanagi Y, Itoh Y and Nakamura T 2019 *Supercond. Sci. Technol.* **32** 065001
[20] Jirsa M, Půst L, Dlouhý D and Koblischka M R 1997 *Phys. Rev.* B **55** 3276–84

[21] Muralidhar M, Sakai N, Jirsa M, Koshizuka N and Murakami M 2004 *Appl. Phys. Lett.* **85** 3504
[22] Kii T *et al* 2012 *IEEE Trans. Appl. Supercond.* **22** 4100904